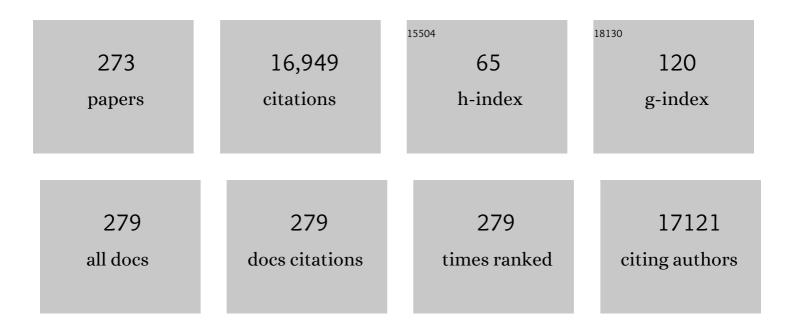
## Craig R Malloy

List of Publications by Year in descending order

Source: https://exaly.com/author-pdf/36917/publications.pdf Version: 2024-02-01



#	Article	IF	CITATIONS
1	Lactate Metabolism in Human Lung Tumors. Cell, 2017, 171, 358-371.e9.	28.9	899
2	Metabolic Heterogeneity in Human Lung Tumors. Cell, 2016, 164, 681-694.	28.9	830
3	2-hydroxyglutarate detection by magnetic resonance spectroscopy in IDH-mutated patients with gliomas. Nature Medicine, 2012, 18, 624-629.	30.7	711
4	Analysis of Cancer Metabolism by Imaging Hyperpolarized Nuclei: Prospects for Translation to Clinical Research. Neoplasia, 2011, 13, 81-97.	5.3	623
5	A roadmap for interpreting 13 C metabolite labeling patterns from cells. Current Opinion in Biotechnology, 2015, 34, 189-201.	6.6	513
6	Transcardiac serotonin concentration is increased in selected patients with limiting angina and complex coronary lesion morphology Circulation, 1989, 79, 116-124.	1.6	487
7	Analysis of Tumor Metabolism Reveals Mitochondrial Glucose Oxidation in Genetically Diverse Human Glioblastomas in the Mouse Brain InÂVivo. Cell Metabolism, 2012, 15, 827-837.	16.2	459
8	MRI detection of glycogen in vivo by using chemical exchange saturation transfer imaging (glycoCEST). Proceedings of the National Academy of Sciences of the United States of America, 2007, 104, 4359-4364.	7.1	370
9	Composition of adipose tissue and marrow fat in humans by 1H NMR at 7 Tesla. Journal of Lipid Research, 2008, 49, 2055-2062.	4.2	320
10	Mitochondrial metabolism mediates oxidative stress and inflammation in fatty liver. Journal of Clinical Investigation, 2015, 125, 4447-4462.	8.2	320
11	Hyperpolarized 13C MRI: Path to Clinical Translation in Oncology. Neoplasia, 2019, 21, 1-16.	5.3	316
12	Effect of metoprolol on myocardial function and energetics in patients with nonischemic dilated cardiomyopathy: A randomized, double-blind, placebo-controlled study. Journal of the American College of Cardiology, 1994, 24, 1310-1320.	2.8	297
13	Metabolism of [Uâ€ <sup>13</sup> C]glucose in human brain tumors <i>in vivo</i> . NMR in Biomedicine, 2012, 25, 1234-1244.	2.8	282
14	Hyperpolarized <sup>13</sup> C allows a direct measure of flux through a single enzyme-catalyzed step by NMR. Proceedings of the National Academy of Sciences of the United States of America, 2007, 104, 19773-19777.	7.1	266
15	Cardioprotective effects of 70-kDa heat shock protein in transgenic mice Proceedings of the National Academy of Sciences of the United States of America, 1996, 93, 2339-2342.	7.1	249
16	Effect of beta-adrenergic blockade on myocardial function and energetics in congestive heart failure. Improvements in hemodynamic, contractile, and diastolic performance with bucindolol Circulation, 1990, 82, 473-483.	1.6	244
17	Responsive MRI Agents for Sensing Metabolism <i>in Vivo</i> . Accounts of Chemical Research, 2009, 42, 948-957.	15.6	243
18	Cytosolic Phosphoenolpyruvate Carboxykinase Does Not Solely Control the Rate of Hepatic Gluconeogenesis in the Intact Mouse Liver. Cell Metabolism, 2007, 5, 313-320.	16.2	232

#	Article	IF	CITATIONS
19	Assessing Cardiac Metabolism. Circulation Research, 2016, 118, 1659-1701.	4.5	211
20	lsotope Tracing of Human Clear Cell Renal Cell Carcinomas Demonstrates Suppressed Glucose Oxidation InÂVivo. Cell Metabolism, 2018, 28, 793-800.e2.	16.2	193
21	MRI Thermometry Based on PARACEST Agents. Journal of the American Chemical Society, 2005, 127, 17572-17573.	13.7	168
22	Left ventricular volumes measured by MR imaging Radiology, 1985, 156, 717-719.	7.3	165
23	Prospective Longitudinal Analysis of 2-Hydroxyglutarate Magnetic Resonance Spectroscopy Identifies Broad Clinical Utility for the Management of Patients With <i>IDH</i> -Mutant Glioma. Journal of Clinical Oncology, 2016, 34, 4030-4039.	1.6	157
24	Carbon flux through citric acid cycle pathways in perfused heart by13C NMR spectroscopy. FEBS Letters, 1987, 212, 58-62.	2.8	153
25	Contribution of exogenous substrates to acetyl coenzyme A: measurement by carbon-13 NMR under non-steady-state conditions. Biochemistry, 1990, 29, 6756-6761.	2.5	145
26	Impaired Tricarboxylic Acid Cycle Activity in Mouse Livers Lacking Cytosolic Phosphoenolpyruvate Carboxykinase. Journal of Biological Chemistry, 2004, 279, 48941-48949.	3.4	141
27	The metabolic state of the rat liver in vivo measured by 31P-NMR spectroscopy. Biochimica Et Biophysica Acta - Molecular Cell Research, 1986, 885, 1-11.	4.1	134
28	Mitochondrial substrate utilization regulates cardiomyocyte cell-cycle progression. Nature Metabolism, 2020, 2, 167-178.	11.9	131
29	Flux through hepatic pyruvate carboxylase and phosphoenolpyruvate carboxykinase detected by hyperpolarized <sup>13</sup> C magnetic resonance. Proceedings of the National Academy of Sciences of the United States of America, 2011, 108, 19084-19089.	7.1	129
30	In vivo measurement of myocardial mass using nuclear magnetic resonance imaging. Journal of the American College of Cardiology, 1986, 8, 113-117.	2.8	123
31	Tm(DOTP)5â^': A23Na+ shift agent for perfused rat hearts. Magnetic Resonance in Medicine, 1990, 15, 25-32.	3.0	123
32	MOXI Is a Mitochondrial Micropeptide That Enhances Fatty Acid Î <sup>2</sup> -Oxidation. Cell Reports, 2018, 23, 3701-3709.	6.4	118
33	Gadolinium-DTPA-enhanced nuclear magnetic resonance imaging of reperfused myocardium: Identification of the myocardial bed at risk. Journal of the American College of Cardiology, 1988, 12, 1064-1072.	2.8	115
34	Influence of global ischemia on intracellular sodium in the perfused rat heart. Magnetic Resonance in Medicine, 1990, 15, 33-44.	3.0	112
35	An integrated <sup>2</sup> H and <sup>13</sup> C NMR study of gluconeogenesis and TCA cycle flux in humans. American Journal of Physiology - Endocrinology and Metabolism, 2001, 281, E848-E856.	3.5	108
36	C-NMR: a simple yet comprehensive method for analysis of intermediary metabolism. Trends in Biochemical Sciences, 1991, 16, 5-10.	7.5	105

#	Article	IF	CITATIONS
37	The Greater Contribution of Gluconeogenesis to Glucose Production in Obesity Is Related to Increased Whole-Body Protein Catabolism. Diabetes, 2006, 55, 675-681.	0.6	105
38	Substrate selection in the isolated working rat heart: effects of reperfusion, afterload, and concentration. Basic Research in Cardiology, 1995, 90, 388-396.	5.9	104
39	Mechanisms by Which Liver-Specific PEPCK Knockout Mice Preserve Euglycemia During Starvation. Diabetes, 2003, 52, 1649-1654.	0.6	103
40	Comparison of kinetic models for analysis of pyruvateâ€ŧoâ€ŀactate exchange by hyperpolarized <sup>13</sup> C NMR. NMR in Biomedicine, 2012, 25, 1286-1294.	2.8	100
41	Diminished Hepatic Gluconeogenesis via Defects in Tricarboxylic Acid Cycle Flux in Peroxisome Proliferator-activated Receptor γ Coactivator-1α (PGC-1α)-deficient Mice*. Journal of Biological Chemistry, 2006, 281, 19000-19008.	3.4	99
42	Improved in vivo magnetic resonance imaging of acute myocardial infarction after intravenous paramagnetic contrast agent administration. American Journal of Cardiology, 1986, 57, 864-868.	1.6	98
43	Glucose production, gluconeogenesis, and hepatic tricarboxylic acid cycle fluxes measured by nuclear magnetic resonance analysis of a single glucose derivative. Analytical Biochemistry, 2004, 327, 149-155.	2.4	97
44	Inhibition of cardiac lipoprotein utilization by transgenic overexpression of Angptl4 in the heart. Proceedings of the National Academy of Sciences of the United States of America, 2005, 102, 1767-1772.	7.1	96
45	Impact of Gd <sup>3+</sup> on DNP of [1- <sup>13</sup> C]Pyruvate Doped with Trityl OX063, BDPA, or 4-Oxo-TEMPO. Journal of Physical Chemistry A, 2012, 116, 5129-5138.	2.5	96
46	Gated sodium-23 nuclear magnetic resonance images of an isolated perfused working rat heart. Science, 1981, 212, 935-936.	12.6	92
47	Ultraâ€short echo time (UTE) MR imaging of the lung: Comparison between normal and emphysematous lungs in mutant mice. Journal of Magnetic Resonance Imaging, 2010, 32, 326-333.	3.4	87
48	DNP by Thermal Mixing under Optimized Conditions Yields >60 000-fold Enhancement of <sup>89</sup> Y NMR Signal. Journal of the American Chemical Society, 2011, 133, 8673-8680.	13.7	86
49	Effect of fasting and acute ethanol administration on the energy state of in vivo liver as measured by 31P-NMR spectroscopy. Biochimica Et Biophysica Acta - Molecular Cell Research, 1986, 885, 12-22.	4.1	85
50	Inhibition of carbohydrate oxidation during the first minute of reperfusion after brief ischemia: NMR detection of hyperpolarized <sup>13</sup> CO <sub>2</sub> and H <sup>13</sup> CO. Magnetic Resonance in Medicine, 2008, 60, 1029-1036.	3.0	85
51	Measurement of gluconeogenesis and pyruvate recycling in the rat liver: a simple analysis of glucose and glutamate isotopomers during metabolism of [1,2,3-13C3]propionate. FEBS Letters, 1997, 412, 131-137.	2.8	84
52	Magnetic resonance imaging of acute myocardial infarction: gadolinium diethylenetriamine pentaacetic acid as a marker of reperfusion Circulation, 1986, 74, 1434-1440.	1.6	83
53	Heptanoate as a Neural Fuel: Energetic and Neurotransmitter Precursors in Normal and Glucose Transporter I-Deficient (G1D) Brain. Journal of Cerebral Blood Flow and Metabolism, 2013, 33, 175-182.	4.3	83
54	<sup>31</sup> Pâ€MRS of healthy human brain: ATP synthesis, metabolite concentrations, pH, and <i>T</i> <sub>1</sub> relaxation times. NMR in Biomedicine, 2015, 28, 1455-1462.	2.8	83

#	Article	IF	CITATIONS
55	Effects of bucindolol on neurohormonal activation in congestive heart failure. American Journal of Cardiology, 1991, 67, 67-73.	1.6	82
56	Electron spin resonance studies of trityl OX063 at a concentration optimal for DNP. Physical Chemistry Chemical Physics, 2013, 15, 9800.	2.8	81
57	Channeling of TCA cycle intermediates in cultured Saccharomyces cerevisiae. Biochemistry, 1990, 29, 9106-9110.	2.5	79
58	<scp>MED</scp> 13â€dependent signaling from the heart confers leanness by enhancing metabolism in adipose tissue and liver. EMBO Molecular Medicine, 2014, 6, 1610-1621.	6.9	77
59	Contribution of various substrates to total citric acid cycle flux and ]anaplerosis as determined by13C isotopomer analysis and O2 consumption in the heart. Magnetic Resonance Materials in Physics, Biology, and Medicine, 1996, 4, 35-46.	2.0	76
60	Imaging the tissue distribution of glucose in livers using a PARACEST sensor. Magnetic Resonance in Medicine, 2008, 60, 1047-1055.	3.0	76
61	A comparative study of short―and longâ€TE <sup>1</sup> H MRS at 3 T for <i>in vivo</i> detection of 2â€hydroxyglutarate in brain tumors. NMR in Biomedicine, 2013, 26, 1242-1250.	2.8	73
62	BDPA: An Efficient Polarizing Agent for Fast Dissolution Dynamic Nuclear Polarization NMR Spectroscopy. Chemistry - A European Journal, 2011, 17, 10825-10827.	3.3	72
63	Detection and localization of recent myocardial infarction by magnetic resonance imaging. American Journal of Cardiology, 1986, 58, 214-219.	1.6	71
64	13C Isotopomer Analysis of Glutamate by Tandem Mass Spectrometry. Analytical Biochemistry, 2002, 300, 192-205.	2.4	71
65	Direct Evidence That Perhexiline Modifies Myocardial Substrate Utilization from Fatty Acids to Lactate. Journal of Cardiovascular Pharmacology, 1995, 25, 469-472.	1.9	70
66	In vivo Na-23 MR imaging and spectroscopy of rat brain during TmDOTP5â^' infusion. Journal of Magnetic Resonance Imaging, 1992, 2, 385-391.	3.4	69
67	Kinetic Modeling and Constrained Reconstruction of Hyperpolarized [1-13C]-Pyruvate Offers Improved Metabolic Imaging of Tumors. Cancer Research, 2015, 75, 4708-4717.	0.9	69
68	Glucose metabolism via the pentose phosphate pathway, glycolysis and Krebs cycle in an orthotopic mouse model of human brain tumors. NMR in Biomedicine, 2012, 25, 1177-1186.	2.8	66
69	A New Class of Macrocyclic Lanthanide Complexes for Cell Labeling and Magnetic Resonance Imaging Applications. Journal of the American Chemical Society, 2005, 127, 16178-16188.	13.7	64
70	Hyperpolarized <sup>89</sup> Y Complexes as pH Sensitive NMR Probes. Journal of the American Chemical Society, 2010, 132, 1784-1785.	13.7	64
71	Analytical solutions for 13C isotopomer analysis of complex metabolic conditions: substrate oxidation, multiple pyruvate cycles, and gluconeogenesis. Metabolic Engineering, 2004, 6, 12-24.	7.0	61
72	Effect of exercise on23Na MRI and relaxation characteristics of the human calf muscle. Journal of Magnetic Resonance Imaging, 2000, 11, 532-538.	3.4	59

5

#	Article	IF	CITATIONS
73	Effect of murine strain on metabolic pathways of glucose production after brief or prolonged fasting. American Journal of Physiology - Endocrinology and Metabolism, 2005, 289, E53-E61.	3.5	57
74	Tmdotp5â^' as a23na shift reagent for thein vivo rat kidney. Magnetic Resonance in Medicine, 1995, 34, 25-31.	3.0	56
75	Competition of pyruvate with physiological substrates for oxidation by the heart: implications for studies with hyperpolarized [1- <sup>13</sup> C]pyruvate. American Journal of Physiology - Heart and Circulatory Physiology, 2010, 298, H1556-H1564.	3.2	56
76	Real-time Detection of Hepatic Gluconeogenic and Glycogenolytic States Using Hyperpolarized [2-13C]Dihydroxyacetone. Journal of Biological Chemistry, 2014, 289, 35859-35867.	3.4	55
77	Quantifying tracer levels of2H2O enrichment from microliter amounts of plasma and urine by2H NMR. Magnetic Resonance in Medicine, 2001, 45, 156-158.	3.0	53
78	Noninvasive evaluation of liver metabolism by 2H and 13C NMR isotopomer analysis of human urine. Analytical Biochemistry, 2003, 312, 228-234.	2.4	53
79	Brain metabolism modulates neuronal excitability in a mouse model of pyruvate dehydrogenase deficiency. Science Translational Medicine, 2019, 11, .	12.4	53
80	Hyperpolarized89Y Offers the Potential of Direct Imaging of Metal Ions in Biological Systems by Magnetic Resonance. Journal of the American Chemical Society, 2007, 129, 12942-12943.	13.7	50
81	Effect of ischemia on NMR detection of phosphorylated metabolites in the intact rat heart. Biochemistry, 1989, 28, 5323-5326.	2.5	49
82	In vivo determination of human breast fat composition by <sup>1</sup> H magnetic resonance spectroscopy at 7 T. Magnetic Resonance in Medicine, 2012, 67, 20-26.	3.0	49
83	Simultaneous Steady-state and Dynamic 13C NMR Can Differentiate Alternative Routes of Pyruvate Metabolism in Living Cancer Cells. Journal of Biological Chemistry, 2014, 289, 6212-6224.	3.4	49
84	Mitochondrial Substrate Utilization Regulates Cardiomyocyte Cell Cycle Progression. Nature Metabolism, 2020, 2, 167-178.	11.9	49
85	Nuclear magnetic resonance imaging in Marfan's syndrome. Journal of the American College of Cardiology, 1987, 9, 70-74.	2.8	48
86	Alterations in substrate utilization in the reperfused myocardium: a direct analysis by carbon-13 NMR. Biochemistry, 1992, 31, 4833-4837.	2.5	47
87	A noninvasive assessment of myocardial oxygen tension:19f nmr spectroscopy of sequestered perfluorocarbon emulsion. Magnetic Resonance in Medicine, 1992, 27, 310-317.	3.0	47
88	Measurement of glycine in the human brain in vivo by <sup>1</sup> Hâ€MRS at 3 T: application in brain tumors. Magnetic Resonance in Medicine, 2011, 66, 609-618.	3.0	44
89	Effects of visceral adiposity on glycerol pathways in gluconeogenesis. Metabolism: Clinical and Experimental, 2017, 67, 80-89.	3.4	43
90	Lactate Dehydrogenase A Governs Cardiac Hypertrophic Growth in Response to Hemodynamic Stress. Cell Reports, 2020, 32, 108087.	6.4	43

#	Article	IF	CITATIONS
91	Energetics and metabolism in the failing heart: important but poorly understood. Current Opinion in Clinical Nutrition and Metabolic Care, 2010, 13, 458-465.	2.5	41
92	Metabolism of hyperpolarized [1â€ <sup>13</sup> C]pyruvate through alternate pathways in rat liver. NMR in Biomedicine, 2016, 29, 466-474.	2.8	41
93	Could <sup>13</sup> C MRI assist clinical decisionâ€making for patients with heart disease?. NMR in Biomedicine, 2011, 24, 973-979.	2.8	40
94	Analysis of gluconeogenic pathways in vivo by distribution of 2H in plasma glucose: comparison of nuclear magnetic resonance and mass spectrometry. Analytical Biochemistry, 2003, 318, 321-324.	2.4	39
95	Quantitation of intracellular [Na <sup>+</sup> ] in vivo by using TmDOTP <sup>5â^'</sup> as an NMR shift reagent and extracellular marker. Jou 1998, 85, 1806-1812.	ırna <b>d.o</b> f Ap	pliedsPhysiol
96	<sup>1</sup> H MRS of intramyocellular lipids in soleus muscle at 7 T: Spectral simplification by using long echo times without water suppression. Magnetic Resonance in Medicine, 2010, 64, 662-671.	3.0	38
97	Differing mechanisms of hepatic glucose overproduction in triiodothyronine-treated rats vs. Zucker diabetic fatty rats by NMR analysis of plasma glucose. American Journal of Physiology - Endocrinology and Metabolism, 2005, 288, E654-E662.	3.5	37
98	Glycine by MR spectroscopy is an imaging biomarker of glioma aggressiveness. Neuro-Oncology, 2020, 22, 1018-1029.	1.2	37
99	Orientation-Conserved Transfer of Symmetric Krebs Cycle Intermediates in Mammalian Tissue. Biochemistry, 1994, 33, 6268-6275.	2.5	36
100	Storage and oxidation of long-chain fatty acids in the C57/BL6 mouse heart as measured by NMR spectroscopy. FEBS Letters, 2006, 580, 4282-4287.	2.8	36
101	The effect of <sup>13</sup> C enrichment in the glassing matrix on dynamic nuclear polarization of [1- <sup>13</sup> C]pyruvate. Physics in Medicine and Biology, 2011, 56, N85-N92.	3.0	36
102	Effects of insulin and cytosolic redox state on glucose production pathways in the isolated perfused mouse liver measured by integrated 2H and 13C NMR. Biochemical Journal, 2006, 394, 465-473.	3.7	35
103	Hyperpolarized <sup>13</sup> C NMR detects rapid drugâ€induced changes in cardiac metabolism. Magnetic Resonance in Medicine, 2015, 74, 312-319.	3.0	35
104	Dynamic monitoring of carnitine and acetylcarnitine in the trimethylamine signal after exercise in human skeletal muscle by 7T <sup>1</sup> Hâ€MRS. Magnetic Resonance in Medicine, 2013, 69, 7-17.	3.0	34
105	Measurement of Hepatic Glucose Output, Krebs Cycle, and Gluconeogenic Fluxes by NMR Analysis of a Single Plasma Glucose Sample. Analytical Biochemistry, 1998, 263, 39-45.	2.4	33
106	Pentose phosphate pathway activity parallels lipogenesis but not antioxidant processes in rat liver. American Journal of Physiology - Endocrinology and Metabolism, 2018, 314, E543-E551.	3.5	33
107	Effects of amino acids on substrate selection, anaplerosis, and left ventricular function in the ischemic reperfused rat heart Journal of Clinical Investigation, 1993, 92, 831-839.	8.2	33
108	Oxidation of lactate and acetate in rat skeletal muscle: analysis by <sup>13</sup> C-nuclear magnetic resonance spectroscopy. Journal of Applied Physiology, 1997, 83, 32-39.	2.5	32

#	Article	IF	CITATIONS
109	Increased Hepatic Fructose 2,6-Bisphosphate after an Oral Glucose Load Does Not Affect Gluconeogenesis. Journal of Biological Chemistry, 2003, 278, 28427-28433.	3.4	32
110	Hepatic glucose production pathways after three days of a high-fat diet. Metabolism: Clinical and Experimental, 2013, 62, 152-162.	3.4	32
111	<sup>13</sup> C NMR measurements of human gluconeogenic fluxes after ingestion of [U- <sup>13</sup> C]propionate, phenylacetate, and acetaminophen. American Journal of Physiology - Endocrinology and Metabolism, 1998, 275, E843-E852.	3.5	30
112	Alterations in hepatic glucose and energy metabolism as a result of calorie and carbohydrate restriction. Hepatology, 2008, 48, 1487-1496.	7.3	30
113	Fast Dissolution Dynamic Nuclear Polarization NMR of 13C-Enriched 89Y-DOTA Complex: Experimental and Theoretical Considerations. Applied Magnetic Resonance, 2012, 43, 69-79.	1.2	30
114	Influence of propranolol on acidosis and high energy phosphates in ischaemic myocardium of the rabbit. Cardiovascular Research, 1986, 20, 710-720.	3.8	29
115	NMR indirect detection of glutamate to measure citric acid cycle flux in the isolated perfused mouse heart. FEBS Letters, 2001, 505, 163-167.	2.8	29
116	Measuring in-vivo metabolism using nuclear magnetic resonance. Current Opinion in Clinical Nutrition and Metabolic Care, 2003, 6, 501-509.	2.5	28
117	Dissolution DNP-NMR spectroscopy using galvinoxyl as a polarizing agent. Journal of Magnetic Resonance, 2013, 227, 14-19.	2.1	28
118	Quantitation of Gluconeogenesis by 2H Nuclear Magnetic Resonance Analysis of Plasma Glucose Following Ingestion of 2H2O. Analytical Biochemistry, 2000, 277, 121-126.	2.4	27
119	13C Isotopomer Analysis of Glutamate by J-Resolved Heteronuclear Single Quantum Coherence Spectroscopy. Analytical Biochemistry, 2001, 289, 187-195.	2.4	27
120	Compartmentation of glycolysis and glycogenolysis in the perfused rat heart. NMR in Biomedicine, 2004, 17, 51-59.	2.8	27
121	Active transport and inotropic state in guinea pig left atrium Circulation Research, 1983, 52, 411-422.	4.5	26
122	Sources of acetyl-CoA entering the tricarboxylic acid cycle as determined by analysis of succinate carbon-13 isotopomers. Biochemistry, 1993, 32, 12240-12244.	2.5	26
123	Dipolar cross-relaxation modulates signal amplitudes in the 1H NMR spectrum of hyperpolarized [13C]formate. Journal of Magnetic Resonance, 2007, 189, 280-285.	2.1	26
124	Influence of Liver Triglycerides on Suppression of Glucose Production by Insulin in Men. Journal of Clinical Endocrinology and Metabolism, 2015, 100, 235-243.	3.6	26
125	Spatial localization of high resolution 31P spectra with a surface coil. Journal of Magnetic Resonance, 1983, 55, 164-169.	0.5	25
126	Determination of Acetyl-CoA Enrichment in Rat Heart and Skeletal Muscle by1H Nuclear Magnetic Resonance Analysis of Glutamate in Tissue Extracts. Analytical Biochemistry, 1997, 249, 201-206.	2.4	25

#	Article	IF	CITATIONS
127	Interaction between the Pentose Phosphate Pathway and Gluconeogenesis from Glycerol in the Liver. Journal of Biological Chemistry, 2014, 289, 32593-32603.	3.4	25
128	Oxidation of [Uâ€ <sup>13</sup> C]glucose in the human brain at 7T under steady state conditions. Magnetic Resonance in Medicine, 2017, 78, 2065-2071.	3.0	25
129	Clinical and hemodynamic characteristics of patients with inducible pulsus alternans. American Heart Journal, 1988, 115, 1251-1257.	2.7	24
130	13C isotopomer analysis of glutamate by heteronuclear multiple quantum coherence-total correlation spectroscopy (HMQC-TOCSY). FEBS Letters, 1998, 440, 382-386.	2.8	24
131	Glucose production pathways by2H and13C NMR in patients with HIV-associated lipoatrophy. Magnetic Resonance in Medicine, 2004, 51, 649-654.	3.0	24
132	Orientation of lipid strands in the extracellular compartment of muscle: Effect on quantitation of intramyocellular lipids. Magnetic Resonance in Medicine, 2009, 61, 16-21.	3.0	24
133	Modeling of Brain Metabolism and Pyruvate Compartmentation Using <sup>13</sup> C NMR <i>in Vivo:</i> Caution Required. Journal of Cerebral Blood Flow and Metabolism, 2013, 33, 1160-1167.	4.3	24
134	Exchange kinetics by inversion transfer: Integrated analysis of the phosphorus metabolite kinetic exchanges in resting human skeletal muscle at 7 T. Magnetic Resonance in Medicine, 2015, 73, 1359-1369.	3.0	24
135	A novel inhibitor of pyruvate dehydrogenase kinase stimulates myocardial carbohydrate oxidation in diet-induced obesity. Journal of Biological Chemistry, 2018, 293, 9604-9613.	3.4	24
136	Assessing the pentose phosphate pathway using [2, 3â€ <sup>13</sup> C <sub>2</sub> ]glucose. NMR in Biomedicine, 2019, 32, e4096.	2.8	24
137	Novel application of complementary imaging techniques to examine in vivo glucose metabolism in the kidney. American Journal of Physiology - Renal Physiology, 2016, 310, F717-F725.	2.7	23
138	Unveiling a hidden <sup>31</sup> P signal coresonating with extracellular inorganic phosphate by outerâ€volumeâ€suppression and localized <sup>31</sup> P MRS in the human brain at 7T. Magnetic Resonance in Medicine, 2018, 80, 1289-1297.	3.0	23
139	PKM1 Exerts Critical Roles in Cardiac Remodeling Under Pressure Overload in the Heart. Circulation, 2021, 144, 712-727.	1.6	23
140	Use of a single 13C NMR resonance of glutamate for measuring oxygen consumption in tissue. American Journal of Physiology - Endocrinology and Metabolism, 1999, 277, E1111-E1121.	3.5	22
141	Comparison of [3,4-13C2]glucose to [6,6-2H2]glucose as a tracer for glucose turnover by nuclear magnetic resonance. Magnetic Resonance in Medicine, 2005, 53, 1479-1483.	3.0	22
142	Metabolism of Glycerol, Glucose, and Lactate in the Citric Acid Cycle Prior to Incorporation into Hepatic Acylglycerols. Journal of Biological Chemistry, 2013, 288, 14488-14496.	3.4	22
143	A new technique for cannulation of the coronary sinus from the femoral vein. Catheterization and Cardiovascular Diagnosis, 1986, 12, 426-429.	0.3	21
144	Dy(DOTP)5â^': A new, stable 23Na shift reagent. Journal of Magnetic Resonance, 1988, 76, 528-533.	0.5	21

#	Article	IF	CITATIONS
145	Quadrature transmit coil for breast imaging at 7 tesla using forced current excitation for improved homogeneity. Journal of Magnetic Resonance Imaging, 2014, 40, 1165-1173.	3.4	21
146	Hyperpolarized δâ€{1â€ <sup>13</sup> C]gluconolactone as a probe of the pentose phosphate pathway. NMR in Biomedicine, 2017, 30, e3713.	2.8	21
147	Does Tumor FDC-PET Avidity Represent Enhanced Glycolytic Metabolism in Non-Small Cell Lung Cancer?. Annals of Thoracic Surgery, 2020, 109, 1019-1025.	1.3	21
148	Effect of Doxorubicin on Myocardial Bicarbonate Production From Pyruvate Dehydrogenase in Women With Breast Cancer. Circulation Research, 2020, 127, 1568-1570.	4.5	21
149	Is there tight channelling in the tricarboxylic acid cycle metabolon?. Biochemical Society Transactions, 1991, 19, 1002-1005.	3.4	20
150	Direct observation of lactate and alanine by proton double quantum spectroscopy in rat hearts supplied with [3‐13C]pyruvate. FEBS Letters, 1992, 303, 247-250.	2.8	20
151	Effects of ischemia on intracellular sodium and phosphates in the in vivo rat liver. Journal of Applied Physiology, 1996, 81, 1395-1403.	2.5	20
152	Oxidation of acetate in rabbit skeletal muscle: Detection by13C NMR spectroscopyin vivo. Magnetic Resonance in Medicine, 1996, 36, 451-457.	3.0	20
153	A13C isotopomer kinetic analysis of cardiac metabolism: influence of altered cytosolic redox and [Ca2+]o. American Journal of Physiology - Heart and Circulatory Physiology, 2004, 287, H889-H895.	3.2	20
154	Production of hyperpolarized 13CO2 from [1-13C]pyruvate in perfused liver does reflect total anaplerosis but is not a reliable biomarker of glucose production. Metabolomics, 2015, 11, 1144-1156.	3.0	20
155	Reproducibility and Absolute Quantification of Muscle Glycogen in Patients with Glycogen Storage Disease by 13C NMR Spectroscopy at 7 Tesla. PLoS ONE, 2014, 9, e108706.	2.5	20
156	Predicting functional recovery from ischemia in the rat myocardium. Basic Research in Cardiology, 1992, 87, 548-558.	5.9	19
157	In vivo studies of cellular energy state, pH, and sodium in rat liver after thermal injury. Journal of Applied Physiology, 1994, 76, 1507-1511.	2.5	19
158	Effects of glutamate and aspartate on myocardial substrate oxidation during potassium arrest. Journal of Thoracic and Cardiovascular Surgery, 1996, 112, 1651-1660.	0.8	19
159	Propionate stimulates pyruvate oxidation in the presence of acetate. American Journal of Physiology - Heart and Circulatory Physiology, 2014, 307, H1134-H1141.	3.2	19
160	An Oral Load of [13C3]Glycerol and Blood NMR Analysis Detect Fatty Acid Esterification, Pentose Phosphate Pathway, and Glycerol Metabolism through the Tricarboxylic Acid Cycle in Human Liver. Journal of Biological Chemistry, 2016, 291, 19031-19041.	3.4	19
161	Efficient <sup>31</sup> P band inversion transfer approach for measuring creatine kinase activity, ATP synthesis, and molecular dynamics in the human brain at 7 T. Magnetic Resonance in Medicine, 2017, 78, 1657-1666.	3.0	19
162	Effects of Empagliflozin Treatment on Glycerolâ€Derived Hepatic Gluconeogenesis in Adults with Obesity: A Randomized Clinical Trial. Obesity, 2020, 28, 1254-1262.	3.0	19

#	Article	IF	CITATIONS
163	Fatty liver disrupts glycerol metabolism in gluconeogenic and lipogenic pathways in humans. Journal of Lipid Research, 2018, 59, 1685-1694.	4.2	18
164	Relationship between Energetic, Ionic, and Functional Status in the Perfused Rat Heart Following Thermal Injury: A31P and23Na NMR Study. Journal of Surgical Research, 1997, 69, 212-219.	1.6	17
165	Determination of the intracellular sodium concentration in perfused mouse liver by31P and23Na magnetic resonance spectroscopy. Magnetic Resonance in Medicine, 1998, 39, 155-159.	3.0	17
166	Multiple bond13C-13C spin-spin coupling provides complementary information in a13C NMR isotopomer analysis of glutamate. Magnetic Resonance in Medicine, 1999, 42, 197-200.	3.0	17
167	Hepatic gluconeogenesis and Krebs cycle fluxes in a CCl4 model of acute liver failure. NMR in Biomedicine, 2002, 15, 45-51.	2.8	17
168	Quantitative measurement of redox state in human brain by <sup>31</sup> P MRS at 7T with spectral simplification and inclusion of multiple nucleotide sugar components in data analysis. Magnetic Resonance in Medicine, 2020, 84, 2338-2351.	3.0	17
169	Amplification of the effects of magnetization exchange by31P band inversion for measuring adenosine triphosphate synthesis rates in human skeletal muscle. Magnetic Resonance in Medicine, 2015, 74, 1505-1514.	3.0	16
170	Limitations of detection of anaplerosis and pyruvate cycling from metabolism of [1-13C] acetate. Nature Medicine, 2015, 21, 108-109.	30.7	16
171	Remodeling of substrate consumption in the murine sTAC model of heart failure. Journal of Molecular and Cellular Cardiology, 2019, 134, 144-153.	1.9	16
172	Metabolism of hyperpolarized <sup>13</sup> Câ€acetoacetate to βâ€hydroxybutyrate detects realâ€ŧime mitochondrial redox state and dysfunction in heart tissue. NMR in Biomedicine, 2019, 32, e4091.	2.8	16
173	Effects of Dichloroacetate on Mechanical Recovery and Oxidation of Physiologic Substrates After Ischemia and Reperfusion in the Isolated Heart. Journal of Cardiovascular Pharmacology, 1998, 31, 336-344.	1.9	16
174	Even-echo rephasing and constant velocity flow. Magnetic Resonance in Medicine, 1987, 4, 422-430.	3.0	15
175	Multiple quantum filtered23Na NMR spectroscopy of the isolated, perfused rat liver. Magnetic Resonance in Medicine, 1999, 41, 1127-1135.	3.0	15
176	Effects of hypothermia on myocardial substrate selection. Annals of Thoracic Surgery, 2002, 74, 1208-1212.	1.3	15
177	Noninvasive monitoring of lactate dynamics in human forearm muscle after exhaustive exercise by <sup>1</sup> H-magnetic resonance spectroscopy at 7 tesla. Magnetic Resonance in Medicine, 2013, 70, 610-619.	3.0	15
178	Real-time hyperpolarized 13C magnetic resonance detects increased pyruvate oxidation in pyruvate de de de de de dehydrogenase kinase 2/4–double knockout mouse livers. Scientific Reports, 2019, 9, 16480.	3.3	15
179	Imaging Acute Metabolic Changes in Patients with Mild Traumatic Brain Injury Using Hyperpolarized [1-13C]Pyruvate. IScience, 2020, 23, 101885.	4.1	15
180	Does indomethacin attenuate the coronary vasodilatory effect of nitroglycerin?. Journal of the American College of Cardiology, 1984, 4, 1114-1117.	2.8	14

#	Article	IF	CITATIONS
181	NOTPME: A31P NMR probe for measurementof divalent cations in biological systems. FEBS Letters, 1991, 280, 121-124.	2.8	14
182	Influence of Cardiac Pacing on Intracellular Sodium in the Isolated Perfused Rat Heart. Investigative Radiology, 1991, 26, 1079-1082.	6.2	14
183	1H NMR Detection of Lactate and Alanine in Perfused Rat Hearts during Global and Low Pressure Ischemia. Magnetic Resonance in Medicine, 1995, 33, 53-60.	3.0	14
184	Substrate selection early after reperfusion of ischemic regions in the working rabbit heart. Magnetic Resonance in Medicine, 1996, 35, 820-826.	3.0	14
185	Role of Excess Glycogenolysis in Fasting Hyperglycemia Among Pre-Diabetic and Diabetic Zucker (fa/fa) Rats. Diabetes, 2007, 56, 777-785.	0.6	14
186	High-resolution detection of 13C multiplets from the conscious mouse brain by ex vivo NMR spectroscopy. Journal of Neuroscience Methods, 2012, 203, 50-55.	2.5	14
187	A 16-Channel Receive, Forced Current Excitation Dual-Transmit Coil for Breast Imaging at 7T. PLoS ONE, 2014, 9, e113969.	2.5	14
188	Accelerated chemical shift imaging of hyperpolarized <sup>13</sup> C metabolites. Magnetic Resonance in Medicine, 2016, 76, 1033-1038.	3.0	14
189	Effects of deuteration on transamination and oxidation of hyperpolarized 13C-Pyruvate in the isolated heart. Journal of Magnetic Resonance, 2019, 301, 102-108.	2.1	14
190	Right-Shifting the Oxyhemoglobin Dissociation Curve with RSR13: Effects on High-Energy Phosphates and Myocardial Recovery After Low-Flow Ischemia. Journal of Cardiovascular Pharmacology, 1998, 31, 359-363.	1.9	14
191	Effects of different oxidative insults on intermediary metabolism in isolated perfused rat hearts. Free Radical Biology and Medicine, 1996, 20, 515-523.	2.9	13
192	Assessment of hepatic pyruvate carboxylase activity using hyperpolarized [1â€ <sup>13</sup> C]â€ <scp>l</scp> ″actate. Magnetic Resonance in Medicine, 2021, 85, 1175-1182.	3.0	13
193	Cardiac measurement of hyperpolarized <sup>13</sup> C metabolites using metaboliteâ€selective multiâ€echo spiral imaging. Magnetic Resonance in Medicine, 2021, 86, 1494-1504.	3.0	13
194	Anticoagulation with heparin during cardiac catheterization and its reversal by protamine. Catheterization and Cardiovascular Diagnosis, 1987, 13, 16-21.	0.3	12
195	Dissociation of Intracellular Sodium from Contractile State in Guinea-Pig Hearts Treated with Ouabain. Journal of Molecular and Cellular Cardiology, 1998, 30, 639-647.	1.9	12
196	Cortical metabolism in pyruvate dehydrogenase deficiency revealed by ex vivo multiplet 13C NMR of the adult mouse brain. Neurochemistry International, 2012, 61, 1036-1043.	3.8	12
197	Band inversion amplifies <sup>31</sup> P- <sup>31</sup> P nuclear overhauser effects: Relaxation mechanism and dynamic behavior of ATP in the human brain by <sup>31</sup> P MRS at 7 T. Magnetic Resonance in Medicine, 2017, 77, 1409-1418.	3.0	12
198	A simple method to monitor hepatic gluconeogenesis and triglyceride synthesis following oral sugar tolerance test in obese adolescents. American Journal of Physiology - Regulatory Integrative and Comparative Physiology, 2019, 317, R134-R142.	1.8	12

#	Article	IF	CITATIONS
199	Assessment of Rapid Hepatic Glycogen Synthesis in Humans Using Dynamic 13C Magnetic Resonance Spectroscopy. Hepatology Communications, 2020, 4, 425-433.	4.3	12
200	The rate of lactate production from glucose in hearts is not altered by per-deuteration of glucose. Journal of Magnetic Resonance, 2017, 284, 86-93.	2.1	12
201	13C isotopomer analyses in intact tissue using {13C}homonuclear decoupling. Magnetic Resonance in Medicine, 1994, 31, 374-379.	3.0	11
202	A Method for Obtaining 13C Isotopomer Populations in 13C-Enriched Glucose. Analytical Biochemistry, 1994, 217, 148-152.	2.4	11
203	Isotopic methods for probing organization of cellular metabolism. Cell Biochemistry and Function, 1996, 14, 259-268.	2.9	11
204	<sup>15</sup> N arnitine, a novel endogenous hyperpolarized MRI probe with long signal lifetime. Magnetic Resonance in Medicine, 2021, 85, 1814-1820.	3.0	11
205	Analysis of spin-echo rephasing with pulsatile flow in 2D FT magnetic resonance imaging. Magnetic Resonance in Medicine, 1987, 4, 307-322.	3.0	10
206	Evidence for reverse flux through pyruvate kinase in skeletal muscle. American Journal of Physiology - Endocrinology and Metabolism, 2009, 296, E748-E757.	3.5	10
207	Lactate Contributes to Glyceroneogenesis and Glyconeogenesis in Skeletal Muscle by Reversal of Pyruvate Kinase. Journal of Biological Chemistry, 2015, 290, 30486-30497.	3.4	10
208	Conditions for 13C NMR detection of 2-hydroxyglutarate in tissue extracts from isocitrate dehydrogenase-mutated gliomas. Analytical Biochemistry, 2015, 481, 4-6.	2.4	10
209	A Switched-Mode Breast Coil for 7 T MRI Using Forced-Current Excitation. IEEE Transactions on Biomedical Engineering, 2015, 62, 1777-1783.	4.2	10
210	Esterase-Catalyzed Production of Hyperpolarized <sup>13</sup> C-Enriched Carbon Dioxide in Tissues for Measuring pH. ACS Sensors, 2018, 3, 2232-2236.	7.8	10
211	Active pyruvate dehydrogenase and impaired gluconeogenesis in orthotopic hepatomas of rats. Metabolism: Clinical and Experimental, 2019, 101, 153993.	3.4	10
212	Hyperpolarized <sup>13</sup> C MR Spectroscopy Depicts in Vivo Effect of Exercise on Pyruvate Metabolism in Human Skeletal Muscle. Radiology, 2021, 300, 626-632.	7.3	10
213	A randomized clinical trial evaluating the effect of empagliflozin on triglycerides in obese adults: Role of visceral fat. Metabolism Open, 2022, 13, 100161.	2.9	10
214	Sources of plasma glucose by automated bayesian analysis of2H NMR spectra. Magnetic Resonance in Medicine, 2003, 50, 659-663.	3.0	9
215	Trap design and construction for highâ€power multinuclear magnetic resonance experiments. Concepts in Magnetic Resonance Part B, 2016, 46B, 162-168.	0.7	9
216	Intramyocellular lipid excess in the mitochondrial disorder MELAS. Neurology: Genetics, 2017, 3, e160.	1.9	9

#	Article	IF	CITATIONS
217	Preoperative imaging of glioblastoma patients using hyperpolarized 13C pyruvate: Potential role in clinical decision making. Neuro-Oncology Advances, 2021, 3, vdab092.	0.7	9
218	Regulatory Consequences of Organization of Citric Acid Cycle Enzymes. Current Topics in Cellular Regulation, 1992, 33, 249-260.	9.6	9
219	tcaSIM: A Simulation Program for Optimal Design of 13C Tracer Experiments for Analysis of Metabolic Flux by NMR and Mass Spectroscopy. Current Metabolomics, 2019, 6, 176-187.	0.5	9
220	13C NMR measurement of flux through alanine aminotransferase by inversion- and saturation-transfer methods. Journal of Magnetic Resonance, 1985, 64, 243-254.	0.5	8
221	The ratio of acetateâ€ŧoâ€glucose oxidation in astrocytes from a single <sup>13</sup> C <scp>NMR</scp> spectrum of cerebral cortex. Journal of Neurochemistry, 2015, 132, 99-109.	3.9	8
222	A simple approach to evaluate the kinetic rate constant for ATP synthesis in resting human skeletal muscle at 7 T. NMR in Biomedicine, 2016, 29, 1240-1248.	2.8	8
223	Measurement of <sup>13</sup> C turnover into glutamate and glutamine pools in brain tumor patients. FEBS Letters, 2017, 591, 3548-3554.	2.8	8
224	Characterization and compensation of inhomogeneity artifact in spiral hyperpolarized <sup>13</sup> C imaging of the human heart. Magnetic Resonance in Medicine, 2021, 86, 157-166.	3.0	8
225	Formation of carbamates of taurine and other amino acids during neutralization of tissue extracts with potassium carbonate/ bicarbonate. Journal of Magnetic Resonance, 1990, 89, 391-398.	0.5	7
226	Effects of oxidant exposure on substrate utilization and high-energy phosphates in isolated rat hearts Circulation Research, 1994, 75, 97-104.	4.5	7
227	The determination of magnesium in human blood plasma by 31P magnetic resonance spectroscopy using a macrocyclic reporter ligand. Biochimica Et Biophysica Acta - General Subjects, 1997, 1336, 434-444.	2.4	7
228	A general chemical shift decomposition method for hyperpolarized <sup>13</sup> C metabolite magnetic resonance imaging. Magnetic Resonance in Chemistry, 2016, 54, 665-673.	1.9	7
229	Hepatic gluconeogenesis influences 13C enrichment in lactate in human brain tumors during metabolism of [1,2-13C]acetate. Neurochemistry International, 2016, 97, 133-136.	3.8	7
230	Automated modification and fusion of voxel models to construct body phantoms with heterogeneous breast tissue: Application to MRI simulations. Journal of Biomedical Graphics and Computing, 2017, 7, 1.	0.2	7
231	Spectral fitting strategy to overcome the overlap between 2â€hydroxyglutarate and lipid resonances at 2.25 ppm. Magnetic Resonance in Medicine, 2021, 86, 1818-1828.	3.0	7
232	13C Isotopomer Analysis of Glutamate A NMR Method to Probe Metabolic Pathways Intersecting in the Citric Acid Cycle. , 2002, , 59-97.		6
233	Modular <sup>31</sup> P wideband inversion transfer for integrative analysis of adenosine triphosphate metabolism, T <sub>1</sub> relaxation and molecular dynamics in skeletal muscle at 7T. Magnetic Resonance in Medicine, 2019, 81, 3440-3452.	3.0	6
234	31 Pâ€MRS of the healthy human brain at 7 T detects multiple hexose derivatives of uridine diphosphate glucose. NMR in Biomedicine, 2021, 34, e4511.	2.8	6

#	Article	IF	CITATIONS
235	Evidence for Transaldolase Activity in the Isolated Heart Supplied with [U-13C3]Glycerol. Journal of Biological Chemistry, 2013, 288, 2914-2922.	3.4	5
236	Advances in Stable Isotope Tracer Methodology Part 1: Hepatic Metabolism via Isotopomer Analysis and Postprandial Lipolysis Modeling. Journal of Investigative Medicine, 2020, 68, 3-10.	1.6	5
237	Co-Polarized [1- <sup>13</sup> C]Pyruvate and [1,3- <sup>13</sup> C <sub>2</sub> ]Acetoacetate Provide a Simultaneous View of Cytosolic and Mitochondrial Redox in a Single Experiment. ACS Sensors, 2021, 6, 3967-3977.	7.8	5
238	Plasma Serotonin Concentrations: Validation of a Sampling Technique Using Long Catheters. American Journal of the Medical Sciences, 1987, 294, 324-327.	1.1	4
239	39K NMR measurement of intracellular potassium during ischemia in the perfused guinea pig heart. Magnetic Resonance in Medicine, 1998, 40, 544-550.	3.0	4
240	Intramyocyte Lipids May Impair Insulin Signaling. American Journal of Psychiatry, 2007, 164, 1475-1475.	7.2	4
241	An Adjustable-Length Dipole Using Forced-Current Excitation for 7T MR. IEEE Transactions on Biomedical Engineering, 2018, 65, 2259-2266.	4.2	4
242	Divergent effects of glutathione depletion on isocitrate dehydrogenase 1 and the pentose phosphate pathway in hamster liver. Physiological Reports, 2020, 8, e14554.	1.7	4
243	13 C NMR of glutamate for monitoring the pentose phosphate pathway in myocardium. NMR in Biomedicine, 2021, 34, e4533.	2.8	4
244	Dualâ€phase imaging of cardiac metabolism using hyperpolarized pyruvate. Magnetic Resonance in Medicine, 2022, 87, 302-311.	3.0	4
245	Dynamic <sup>13</sup> C MR spectroscopy as an alternative to imaging for assessing cerebral metabolism using hyperpolarized pyruvate in humans. Magnetic Resonance in Medicine, 2022, 87, 1136-1149.	3.0	4
246	Effects of storage and reperfusion oxygen content on substrate metabolism in the isolated rat lung. Annals of Thoracic Surgery, 2000, 70, 264-269.	1.3	3
247	Correlation of Cerebral Metabolites With Clinical Outcome Among Patients With Severe Congestive Heart Failure. Circulation, 2001, 103, 2771-2772.	1.6	3
248	Transfer of hyperpolarization from long T1 storage nuclei to short T1 neighbors using FLOPSY-8. Journal of Magnetic Resonance, 2011, 213, 187-191.	2.1	3
249	Carbon-13 Nuclear Magnetic Resonance for Analysis of Metabolic Pathways. , 2013, , 415-445.		3
250	A 32â€channel receive array coil for bilateral breast imaging and spectroscopy at 7T. Magnetic Resonance in Medicine, 2021, 85, 551-559.	3.0	3
251	A 16-Channel <sup>13</sup> C Array Coil for Magnetic Resonance Spectroscopy of the Breast at 7T. IEEE Transactions on Biomedical Engineering, 2021, 68, 2036-2046.	4.2	3
252	Analysis of steady-state carbon tracer experiments using akaike information criteria. Metabolomics, 2021, 17, 61.	3.0	3

#	Article	IF	CITATIONS
253	<sup>13</sup> C‣abeled Diethyl Ketoglutarate Derivatives as Hyperpolarized Probes of 2â€Ketoglutarate Dehydrogenase Activity. Analysis & Sensing, 2021, 1, 156-160.	2.0	3
254	Cardiac Metabolism. , 1994, , 439-449.		3
255	Spatial localization of NMR signal with a passive surface gradient. Journal of Magnetic Resonance, 1988, 80, 364-369.	0.5	2
256	The Cooperative Behavior of Krebs Tricarboxylic Acid Cycle Enzymes. Advances in Molecular and Cell Biology, 1995, 11, 125-145.	0.1	2
257	Metabolic Networks in the Liver by 2H and 13C NMR. , 2005, , 159-174.		2
258	Biochemical Specificity in Human Cardiac Imaging by <sup>13</sup> C Magnetic Resonance Imaging. Circulation Research, 2016, 119, 1146-1148.	4.5	2
259	Magnetic resonance imaging in aortic valve, ascending aortic and isthmic aortic disease. American Journal of Cardiology, 1985, 55, 1243-1244.	1.6	1
260	Reply to: Intramyocellular lipids <i>vs.</i> intramyocellular triglycerides. Magnetic Resonance in Medicine, 2012, 67, 299-299.	3.0	1
261	The presence of 3-hydroxypropionate and 1,3-propanediol suggests an alternative path for conversion of glycerol to Acetyl-CoA. Metabolism Open, 2021, 9, 100086.	2.9	1
262	Imaging Myocardial Metabolism. , 2018, , 243-279.		1
263	IFAC 1994: 13 C NMR Isotopomer Analysis for Investigation of Metabolic Pathways in Intact Tissues. IFAC Postprint Volumes IPPV / International Federation of Automatic Control, 1994, 27, 361-365.	0.4	Ο
264	Are Substrates Channeled In The Krebs Citric Acid Cycle?. Advances in Molecular and Cell Biology, 1996, , 263-271.	0.1	0
265	TCA Cycle Turnover And Serum Glucose Sources By Automated Bayesian Analysis Of NMR Spectra. AIP Conference Proceedings, 2004, , .	0.4	Ο
266	Energetic Adaptations and Stress Reserve in the Obese Heart. Circulation, 2020, 141, 1164-1167.	1.6	0
267	New Insights into Metabolic Regulation from Hyperpolarized 13C MRS/MRI Studies. , 2021, , 181-203.		0
268	Detrimental Role of High Dietary Phosphate Intake on Skeletal Muscle ATP Synthesis in Healthy Humans. FASEB Journal, 2021, 35, .	0.5	0
269	Absolute quantification of muscle glycogen content in patients with glycogen storage disease by 13C NMR spectroscopy at 7 Tesla. FASEB Journal, 2012, 26, 1078.39.	0.5	0
270	X-ray microanalysis of right ventricular guinea pig myocytes for correllation with NMR measurements of intracellular NA changes after ouabain treatment. Proceedings Annual Meeting Electron Microscopy Society of America, 1992, 50, 1582-1583.	0.0	0

#	Article	IF	CITATIONS
271	Substrate Metabolism in the Citric Acid Cycle of the Heart by 13C NMR. , 1993, , 153-168.		0
272	Analysis of Mitochondrial Function by Carbon-13 Nuclear Magnetic Resonance Spectroscopy in Intact Tissues. , 1993, , 127-145.		0
273	Abstract 535: Mathematical Modeling of Hyperpolarized Pyruvate Metabolism in Human Heart. Circulation Research, 2020, 127, .	4.5	0